Published for SISSA by Springer

Received: *February 24, 2015*
Accepted: *April 8, 2015*
Published: *April 28, 2015*

Exclusive photoproduction of charmonia in $\gamma p \to Vp$ and $pp \to pVp$ reactions within k_t-factorization approach

Anna Cisek,[a] **Wolfgang Schäfer**[b] **and Antoni Szczurek**[b,a]

[a] *University of Rzeszów,*
ul. Rejtana 16c, PL-35-959 Rzeszów, Poland
[b] *Institute of Nuclear Physics PAN,*
ul. Radzikowskiego 152, PL-31-342 Kraków, Poland

E-mail: acisek@univ.rzeszow.pl, Wolfgang.Schafer@ifj.edu.pl, Antoni.Szczurek@ifj.edu.pl

Abstract: The amplitude for $\gamma p \to J/\psi p$ ($\gamma p \to \psi' p$) is calculated in a pQCD k_T-factorization approach. The total cross section for this process is calculated for different unintegrated gluon distributions and compared with the HERA data and the data extracted recently by the LHCb collaboration. The amplitude for $\gamma p \to J/\psi p$ ($\gamma p \to \psi' p$) is used to predict the cross section for exclusive photoproduction of J/ψ (ψ') mesons in proton-proton collisions. Compared to earlier calculations we include both Dirac and Pauli electromagnetic form factors. The effect of the Pauli form factor is quantified. We discuss the role of the J/ψ and ψ' $c\bar{c}$ wave functions for differential distributions and corresponding ratios for ψ' and J/ψ. Absorption effects are taken into account and their role is discussed in detail. Different differential distributions e.g. in J/ψ (ψ') rapidity and transverse momentum are presented and compared with existing experimental data. The unintegrated gluon distribution with nonlinear effects built in and Gaussian wave functions better describe recent experimental data of the LHCb collaboration but no definite conclusion on onset of saturation can be drawn. We present our results also for the Tevatron. A good agreement with the CDF experimental data points at the midrapidity for both J/ψ and ψ' is achieved.

Keywords: Hadronic Colliders, QCD Phenomenology

ArXiv ePrint: 1405.2253

Open Access, © The Authors.
Article funded by SCOAP[3].

doi:10.1007/JHEP04(2015)159

Contents

1 Introduction

The exclusive production of J/ψ mesons in proton-proton and proton-antiproton scattering has recently attracted some interest [1–10].

In an early paper [5], it was shown that the exclusive production of J/ψ at the Tevatron is sensitive to the $\gamma p \to J/\psi p$ scattering in the similar region of energy as measured at HERA [11]. Given that fact the measured cross section for $\gamma p \to J/\psi p$ was parametrized and used in that calculation. Our predictions there could be successfully confronted with the Tevatron data [1] and good agreement was achieved [12]. The formalism proposed in [13] and used in [5] allows to calculate fully differential distributions for the three-body reaction in the broad range of four-dimensional phase space. The formalism proposed in [13] allows to test unintegrated gluon distributions (UGDFs) in the proton provided the quark-antiquark wave function of the meson is known. The experimental data for production of different vector mesons prefer Gaussian light-cone wave function [13–16].

Recently also the LHCb collaboration measured rapidity distributions of the J/ψ meson but rather in semi-exclusive reaction [2, 3].[1] Using some theoretical input from ref. [5] the LHCb collaboration tried to extract the cross section for the $\gamma p \to J/\psi p$ reaction at unprecedently high energies not available before at HERA. The procedure proposed uses some assumption which are only approximate and need further verification. Very recently the authors of ref. [10] tried to use the pseudo-data to achieve information on integrated gluon distribution in very small x (longitudinal momentum fraction carried by the gluon) region, not

[1] The protons were not detected and only incomplete rapidity gap was checked.

JHEP04(2015)159

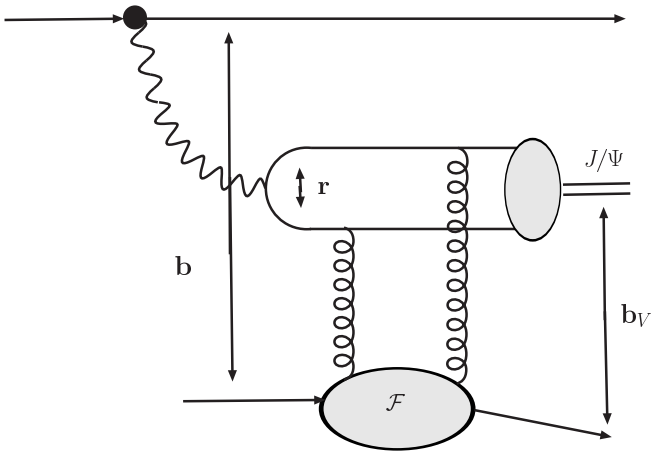

Figure 1. Diagrams representing amplitude for the $\gamma p \to J/\psi$ p process.

available earlier at electron machines. The formalism applied in ref. [10] uses a slightly simplified collinear formalism where the quark-antiquark wave function is replaced by a normalization constant [17]. In this formalism only rapidity distribution was discussed. In contrast to the collinear approach the k_t-factorization approach allows to study the complete kinematically reaction. In the present analysis we shall show how some UGDFs from the literature compare to the LHCb data [2, 3]. We leave the inclusion of the inelastic contribution as well as a possible fitting of UGDF for further sudies. Compared to other calculations in the literature we include here not only the spin-conserving coupling but also the spin-flip one.

2 Photoproduction process $\gamma p \to J/\psi p$

The imaginary part of the forward amplitude sketched in figure 1 can be written as [13, 14]:

$$\Im m\, \mathcal{M}_T(W, \Delta^2 = 0, Q^2 = 0) = W^2 \frac{c_v \sqrt{4\pi\alpha_{em}}}{4\pi^2}\, 2 \int_0^1 \frac{dz}{z(1-z)} \int_0^\infty \pi dk^2 \psi_V(z, k^2)$$
$$\times \int_0^\infty \frac{\pi d\kappa^2}{\kappa^4} \alpha_S(q^2) \mathcal{F}(x_{\rm eff}, \kappa^2) \Big(A_0(z, k^2)\, W_0(k^2, \kappa^2) + A_1(z, k^2)\, W_1(k^2, \kappa^2) \Big) . \quad (2.1)$$

When evaluating the loop diagram, we use a covariant vertex for the $\bar{c}c \to V$ transition, which couples quarks to the pure S-wave state (see e.g. eq. (107 ff.) of ref. [13]. This vertex, derived e.g. in [18, 19] includes all the relativistic effects associated with the spin rotations of quarks, etc. It differs from the γ_μ-vertex, which would contain the admixture of D-waves, and in the context of diffractive vector mesons has been first used in [20].

$$A_0(z, k^2) = m_c^2 + \frac{k^2 m_c}{M + 2m_c} ,$$
$$A_1(z, k^2) = \left[z^2 + (1-z)^2 - (2z-1)^2 \frac{m_c}{M + 2m_c} \right] \frac{k^2}{k^2 + m_c^2} ,$$

JHEP04(2015)159

$$W_0(k^2,\kappa^2) = \frac{1}{k^2+m_c^2} - \frac{1}{\sqrt{(k^2-m_c^2-\kappa^2)^2+4m_c^2k^2}}\,,$$
$$W_1(k^2,\kappa^2) = 1 - \frac{k^2+m_c^2}{2k^2}\left(1+\frac{k^2-m_c^2-\kappa^2}{\sqrt{(k^2-m_c^2-\kappa^2)^2+4m_c^2k^2}}\right).$$

Here $\psi_V(z,k^2)$ is the meson light-cone wave function, $\mathcal{F}(x_{\rm eff},\kappa^2)$ is the unintegrated gluon distribution function. The invariant mass of the $c\bar{c}$-system is given by

$$M = \sqrt{\frac{k^2+m_c^2}{z(1-z)}} \tag{2.2}$$

We choose the scale of the QCD constant running coupling at $q^2 = \max\{\kappa^2, k^2+m_c^2\}$. The full amplitude, at finite momentum transfer is given by:

$$\mathcal{M}(W,\Delta^2) = (i+\rho)\,\Im m\mathcal{M}(W,\Delta^2=0,Q^2=0)\cdot f(\Delta^2,W)\,, \tag{2.3}$$

where the real part of the amplitude is restored from analyticity,

$$\rho = \frac{\Re e\mathcal{M}}{\Im m\mathcal{M}} = \tan\left(\frac{\pi}{2}\frac{\partial\log\left(\Im m\mathcal{M}/W^2\right)}{\partial\log W^2}\right). \tag{2.4}$$

Above the dependence on momentum transfer $t=-\Delta^2$ is parametrized by the function $f(\Delta^2,W)$, which dependence on energy derives from the Regge slope

$$B(W) = b_0 + 2\alpha'_{\rm eff}\log\left(\frac{W^2}{W_0^2}\right), \tag{2.5}$$

with: $b_0 = 4.88$, $\alpha'_{\rm eff} = 0.164\,\mathrm{GeV}^{-2}$ and $W_0 = 90\,\mathrm{GeV}$ [11].

It is customary to parametrize

$$f(t,W) = \exp\left(\frac{1}{2}B(W)t\right), \tag{2.6}$$

which is sufficient for a very good description of experimental data at $|t| \lesssim 0.5\,\mathrm{GeV}^2$.

However, below we are also interested in an intermediate region of $|t| \sim 1 \div 2\,\mathrm{GeV}^2$. In this region, data deviate from the strict exponential behaviour, and it is better to use a "stretched exponential" parametrization

$$f(t,W) = \exp(\mu^2 B(W))\exp\left(-\mu^2 B(W)\sqrt{1-t/\mu^2}\right), \tag{2.7}$$

which at low $|t| \ll \mu^2$ coincides with the exponential form of eq. (2.6), and at larger t features a harder tail. This function is close to a parametrization $\sim\exp(-ap_\perp)$ suggested by Orear [21] for elastic pp-scattering; a similar parametrization has recently been used in [22]. Below, we will refer to it as the "Orear"-parametrization. The free parameter μ has been adjusted to HERA data [23], see figure 2. We find a very good description using $\mu = 0.8\,\mathrm{GeV}$. It is well known, that "stretched exponentials" can arise from a superposition of several exponentials with different slopes. Here one may think, for example of multiple Reggeon/Pomeron exchanges. We also cannot exclude, that the data shown in figure 2 in fact do contain a contamination of dissociative events.

JHEP04(2015)159

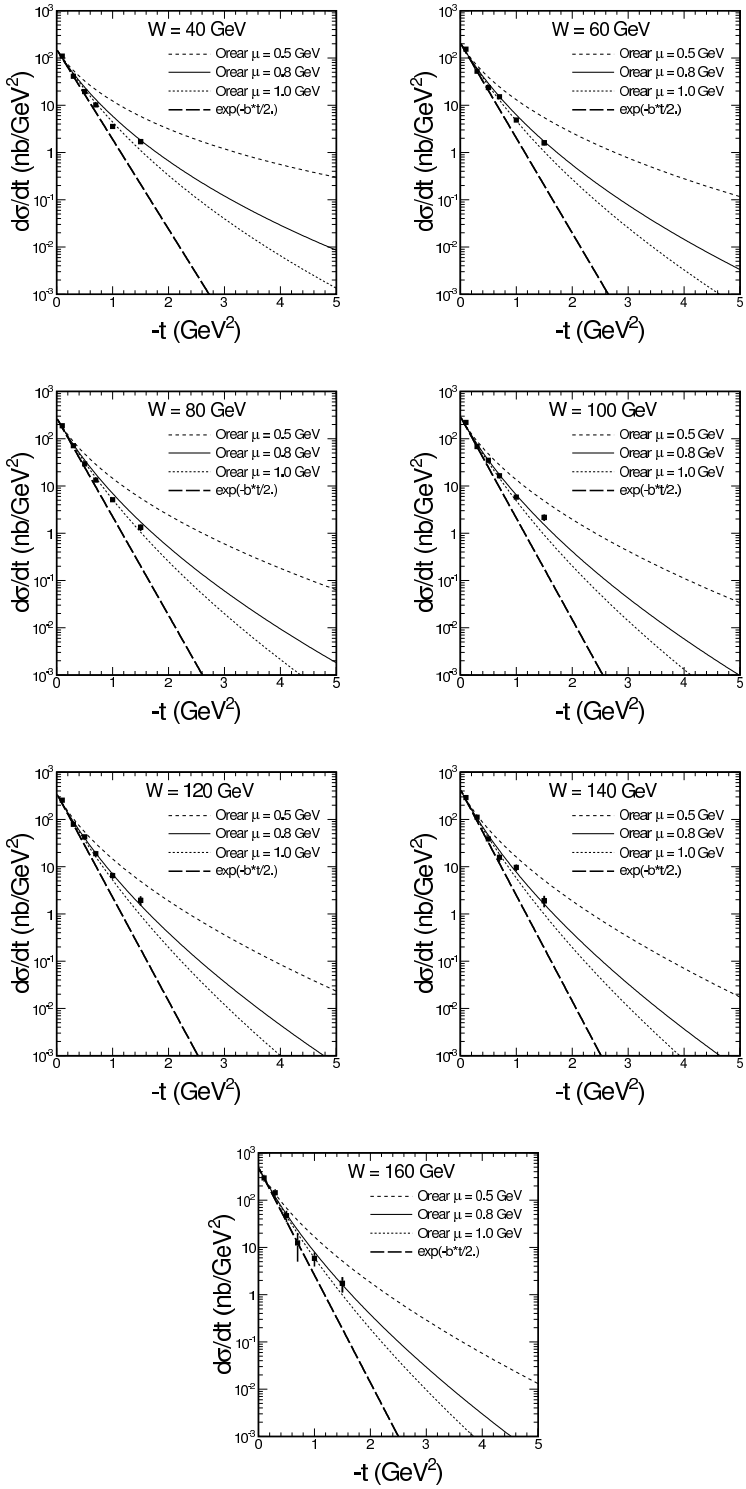

Figure 2. Dependence of the photoproduction cross section on four-momentum squared ($d\sigma/dt$) for different energies indicated in the figure caption.

JHEP04(2015)159

3 J/ψ and ψ' wave functions

We include the Fermi-motion of quark and antiquark in the bound-state by means of the light-cone wave function of the vector meson.

While the light-cone wave function $\psi_V(z, k^2)$ is written as a function of the momentum fraction z of the quark and the relative transverse momentum $\boldsymbol{k}$ of quarks in the bound state, in fact it depends only on the relative momentum $\vec{p}$ of c and $\bar{c}$ in the rest frame of the meson given by

$$\vec{p} = (\boldsymbol{p}, p_z) = (\boldsymbol{k}, (z - 1/2)M) \; . \tag{3.1}$$

Following quite literally the approach of [13, 14] we use as an ansatz for the wave function dependence on $\vec{p}$:

$$\begin{aligned} \psi_{1S}(z, k^2) \; &= \; \psi_{1S}(\vec{p}^{\,2}) = c_1 \, \exp\Big(- a_1^2 \vec{p}^{\,2}/2 \Big) \; , \\ \psi_{2S}(z, k^2) \; &= \; \psi_{2S}(\vec{p}^{\,2}) = c_2 (\xi_{\rm node} - a_2^2 \vec{p}^{\,2}) \, \exp\Big(- a_2^2 \vec{p}^{\,2}/2 \Big) \, . \end{aligned} \tag{3.2}$$

This functional dependence is obviously inspired by the harmonic-oscillator potential, notice however that following [13, 14] we keep a_1, a_2 which would be equal in the strict harmonic oscillator potential as free parameters. The parameters are fixed from the leptonic decay widths of J/ψ and ψ', as well as from the orthonormality conditions of the $1S, 2S$ bound states. Note, that our ansatz 3.2 refers directly to the light-cone wave function of the meson.

Recently a number of theoretical arguments for an effectively harmonic confinement potential on the light-front from various approaches have been given in [24] (see also [25]). A phenomenology of various transitions and decays of $2S$-charmonia in a light-front quark-model using harmonic oscillator-type wave functions can be found in [26]. Ultimately one may want to go beyond the phenomenological approach used here and make parameter-free predictions, in this regard some progress in obtaining directly the light-front wave functions of heavy quarkonia has been made in [27]. We note that the wave functions of [27] are also close to harmonic-oscillator wave functions.

As a second option for the wave function, we adopt one that has only a power-law falloff at large momenta, inspired by the behaviour of a Coulomb bound state. Explicitly, we write

$$\begin{aligned} \psi_{1S}(z, k^2) \; &= \; \psi_{1S}(\vec{p}^{\,2}) = \frac{\tilde{c}_1}{\sqrt{M}} \, \frac{1}{[1 + \tilde{a}_1^2 \vec{p}^{\,2}]^2} \; , \\ \psi_{2S}(z, k^2) \; &= \; \psi_{2S}(\vec{p}^{\,2}) = \frac{\tilde{c}_2}{\sqrt{M}} \, \frac{(\tilde{\xi}_{\rm node} - \tilde{a}_2^2 \vec{p}^{\,2})}{[1 + \tilde{a}_2^2 \vec{p}^{\,2}]^3} \, . \end{aligned} \tag{3.3}$$

Also here we determine parameters $\tilde{c}_{1,2}, \tilde{a}_{1,2}, \tilde{\xi}_{\rm node}$ from decay width and orthonormality. Notice that here $\tilde{c}_{1,2}$ have dimension $\mathrm{GeV}^{1/2}$.

Let us stress that an account of the wave function is important to make predictions for the production of excited charmonium states. While we use the momentum space formulation of diffractive vector meson production, the equivalent color-dipole formulation is more intuitive to understand the argument: it is the overlap of the light-cone wave functions of photon and vector meson which controls the effective dipole size distributions

JHEP04(2015)159

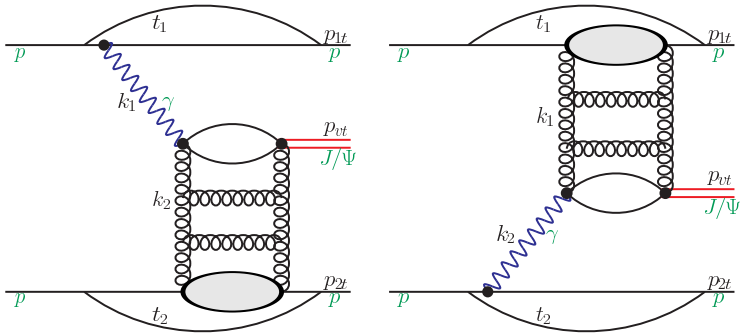

Figure 3. Diagrams representing Born amplitudes considered for the $pp \to ppJ/\psi$ process.

that enter the dipole cross section [28, 29]. Here especially the node in the wave function of the radial excitation has a subtle effect on the energy dependence [30]. For a recent approach to the node-effect in the color-dipole approach, see [31].

Often an extreme nonrelativistic limit is adopted, in which heavy quarks are assumed to be at rest in the meson rest frame, and hence the momentum dependence of the wave function is neglected. Typically then also the transverse momentum of gluons is integrated out [17], and the diffractive amplitude becomes proportional to the integrated glue of the target. Strictly speaking in such an approximation one cannot predict the energy dependence of J/ψ vs. ψ' production, as to the accuracy of [17] it is illegitimate to differentiate between $2m_c$, the invariant mass of the $c\bar{c}$ pair, M, or the bound-state mass M_V, either of which could enter the hard scale. The wave function "node effect" [14, 29], which leads to a strong dependence of the $\psi'/J/\psi$ ratio on the bound-state wave function clearly cannot be accomodated in this way. The importance of relativistic effects had also been stressed in [32], although the precise implementation of Fermi motion differs from the one adopted by us.

4 Exclusive photoproduction of J/ψ in pp and $p\bar{p}$ collisions

The Born mechanism of the production of the J/ψ meson (similar mechanism for ψ') in proton-proton collisions is shown in figure 3. There are two diagrams. In first diagram photon couples to the first proton while in the second diagram the photon couples to the second proton. The photon splits to a $c\bar{c}$ dipole which interacts with the other proton via exchange of gluonic ladder. The presence of two mechanisms leads to interference effects [5]. The interference effect leads to interesting azimuthal correlations between outgoing protons [5], never identified so far.

The full Born amplitude for the $pp \to pVp$ process can be written as:

$$\mathcal{M}^{\lambda_1\lambda_2\to\lambda_1'\lambda_2'\lambda_V}_{h_1h_2\to h_1h_2V}(s,s_1,s_2,t_1,t_2) = \mathcal{M}_{\gamma\mathbb{P}} + \mathcal{M}_{\mathbb{P}\gamma}$$
$$= \langle p_1',\lambda_1'|J_\mu|p_1,\lambda_1\rangle \epsilon^*_\mu(q_1,\lambda_V)\frac{\sqrt{4\pi\alpha_{em}}}{t_1}\mathcal{M}^{\lambda_{\gamma^*}\lambda_2\to\lambda_V\lambda_2}_{\gamma^*h_2\to Vh_2}(s_2,t_2,Q_1^2)$$

JHEP04(2015)159

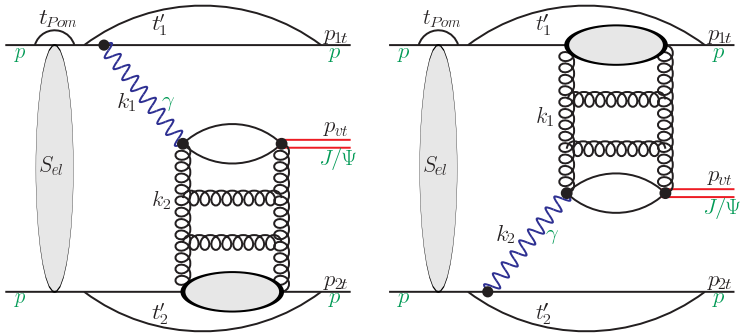

Figure 4. Diagrams representing absorptive corrections considered for the $pp \to ppJ/\psi$ process. Here the momentum transfer squared in the elastic amplitude is $t_{Pom} = -\boldsymbol{k}^2$ from eq. (4.4).

$$+\langle p_2', \lambda_2' | J_\mu | p_2, \lambda_2 \rangle \epsilon_\mu^*(q_2, \lambda_V) \frac{\sqrt{4\pi\alpha_{em}}}{t_2} \mathcal{M}^{\lambda_{\gamma^*}\lambda_1 \to \lambda_V \lambda_1}_{\gamma^* h_1 \to V h_1}(s_1, t_1, Q_2^2) \,. \tag{4.1}$$

In terms of their transverse momenta $\boldsymbol{p}_{1,2}$ the relevant four-momentum transfers squared are $t_1 = -(\boldsymbol{p}_1^2 + z_1^2 m_p^2)/(1-z_1)$ and $t_2 = -(\boldsymbol{p}_2^2 + z_2^2 m_p^2)/(1-z_2)$ and $s_1 \approx (1-z_2)s$ and $s_2 \approx (1-z_1)s$ are the familiar Mandelstam variables.

Then, the amplitude of eq. (4.1) for the emission of a photon of transverse polarization λ_V, and transverse momentum $\boldsymbol{q}_1 = -\boldsymbol{p}_1$ can be written as:

$$\langle p_1', \lambda_1' | J_\mu | p_1, \lambda_1 \rangle \epsilon_\mu^*(q_1, \lambda_V) = \frac{(\boldsymbol{e}^{*(\lambda_V)} \boldsymbol{q}_1)}{\sqrt{1-z_1}} \frac{2}{z_1} \chi_{\lambda'}^\dagger \left\{ F_1(Q_1^2) - \frac{i\kappa_p F_2(Q_1^2)}{2m_p} (\boldsymbol{\sigma}_1 \cdot [\boldsymbol{q}_1, \boldsymbol{n}]) \right\} \chi_\lambda \,. \tag{4.2}$$

Above χ_λ is its spinor, $\boldsymbol{e}^{(\lambda)} = -(\lambda \boldsymbol{e}_x + i \boldsymbol{e}_y)/\sqrt{2}$, $\boldsymbol{n} || \boldsymbol{e}_z$ denotes the collision axis, and $\boldsymbol{\sigma}_1/2$ is the spin operator for nucleon 1. F_1 and F_2 are respectively the Dirac and Pauli electromagnetic form factors, $\kappa_p = 1.79$.

Below the $2 \to 3$ bare amplitude (when absorption effects is ignored) is shown in the form of a 2-dimensional vector:

$$\begin{aligned} \boldsymbol{M}^{(0)}(\boldsymbol{p}_1, \boldsymbol{p}_2) \,=\, & e_1 \frac{2}{z_1} \frac{\boldsymbol{p}_1}{t_1} \mathcal{F}_{\lambda_1' \lambda_1}(\boldsymbol{p}_1, t_1) \mathcal{M}_{\gamma^* h_2 \to V h_2}(s_2, t_2, Q_1^2) \\ & + e_2 \frac{2}{z_2} \frac{\boldsymbol{p}_2}{t_2} \mathcal{F}_{\lambda_2' \lambda_2}(\boldsymbol{p}_2, t_2) \mathcal{M}_{\gamma^* h_1 \to V h_1}(s_1, t_1, Q_2^2) \,. \end{aligned}$$

Because of the presence of the proton from factors only small Q_1^2 and Q_2^2 enter the amplitude for the hadronic process. This means that in practice, inside the photoproduction amplitude, one can put $Q_1^2 = Q_1^2 = 0$.

The full amplitude for the $pp \to pJ/\psi p$ or $pp \to p\psi' p$ reaction is calculated as:

$$\begin{aligned} \boldsymbol{M}(\boldsymbol{p}_1, \boldsymbol{p}_2) \,&=\, \int \frac{d^2\boldsymbol{k}}{(2\pi)^2} \, S_{el}(\boldsymbol{k}) \, \boldsymbol{M}^{(0)}(\boldsymbol{p}_1 - \boldsymbol{k}, \boldsymbol{p}_2 + \boldsymbol{k}) \\ &=\, \boldsymbol{M}^{(0)}(\boldsymbol{p}_1, \boldsymbol{p}_2) - \delta \boldsymbol{M}(\boldsymbol{p}_1, \boldsymbol{p}_2) \,. \end{aligned} \tag{4.3}$$

JHEP04(2015)159

The corresponding diagrams are shown in figure 4. In the present calculations we include only elastic rescattering corrections. Then

$$S_{el}(\boldsymbol{k}) = (2\pi)^2\delta^{(2)}(\boldsymbol{k}) - \frac{1}{2}T(\boldsymbol{k}) \ , \ T(\boldsymbol{k}) = \sigma_{\rm tot}^{pp}(s)\,\exp\left(-\frac{1}{2}B_{el}\boldsymbol{k}^2\right). \tag{4.4}$$

In practical evaluations we take $B_{el} = 17\,\mathrm{GeV}^{-2}$, $\sigma_{\rm tot}^{pp} = 76$ mb [5, 33] for the Tevatron energy and $B_{el} = 19.89\,\mathrm{GeV}^{-2}$, $\sigma_{\rm tot}^{pp} = 98.6$ mb for the LHC energy [34].

The absorptive correction to the amplitude can be written as:

$$\delta\boldsymbol{M}(\boldsymbol{p}_1,\boldsymbol{p}_2) = \int \frac{d^2\boldsymbol{k}}{2(2\pi)^2}\,T(\boldsymbol{k})\,\boldsymbol{M}^{(0)}(\boldsymbol{p}_1-\boldsymbol{k},\boldsymbol{p}_2+\boldsymbol{k})\,.$$

Inelastic intermediate proton excitations can be taken into account effectively by multiplying elastic amplitdes by a constant bigger than 1.

5 Results

5.1 J/ψ production

Before we go to the proton-proton processes let us first summarize our description of HERA data [11, 35, 36]. In figure 5 we show results of calculations with the Ivanov-Nikolaev [13, 37] and Kutak-Staśto [38] gluon unintegrated distributions. In the second case we consider both a BFKL version called linear and a version where gluon is obtained by solving Balitsky-Kovchegov evolution equation called nonlinear. We also show the result for the exponential and Orear t-dependences. The cross sections with Orear t-dependence are larger than those for exponential t-dependence. We wish to empasize in this context that the assumption of exponential slope was used to obtained (integrate) the experimental data. Our estimate shows an error one makes in such a procedure, we caution however that it the Orear parametrization may effectively contain dissociative processes.

In figure 6 we show rapidity distribution in the Born approximation for different UGDFs. The dashed line represents calculation when only vector (F_1) terms are included, while the solid line represents calculations with vector (F_1) and tensor (F_2) couplings of photon to the proton. The effect of taking into account tensor coupling is here of the order of 5 % only.

Similar distributions in J/ψ transverse momentum are shown in figure 7. Large effect of the tensor coupling can be observed at large transverse momenta. At $p_t \sim 3\,\mathrm{GeV}$ we get an enhancement factor of the cross section of order of 10. Large transverse momenta are potentially interesting because of odderon exchange contribution (see e.g. [7]).

The eikonal absorption damps rapidity distribution of J/ψ by about 30 % as is shown in figure 8. The result with the Kutak-Staśto distribution which includes nonlinear effects is almost consistent with the newest LHCb data. Does it mean that we observe an onset of gluon saturation? We shall return to it in a while.

How the absorption modifies the J/ψ transverse momentum distribution is shown in figure 9. The absorption leads to a strong damping at large J/ψ transverse momenta. This overcompensates the effect of inclusion of the tensor electromagnetic coupling quantified by

JHEP04(2015)159

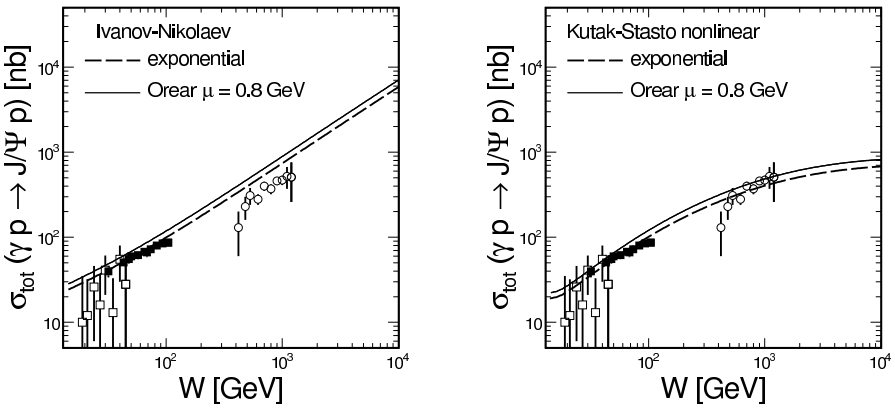

Figure 5. Total cross section for the $\gamma p \to J/\psi p$ as a function of the subsystem energy together with the HERA data and pseudodata obtained by the LHCb collaboration. Here two different UGDFs have been used: Ivanov-Nikolaev (left panel), and Kutak-Stasto nonlinear (right panel). The dashed lines represents calculation with an exponential parametrization of the t-dependence, while the solid line corresponds to the Orear parametrization. The HERA data [11] and the LHCb data [2, 3] are shown for comparison.

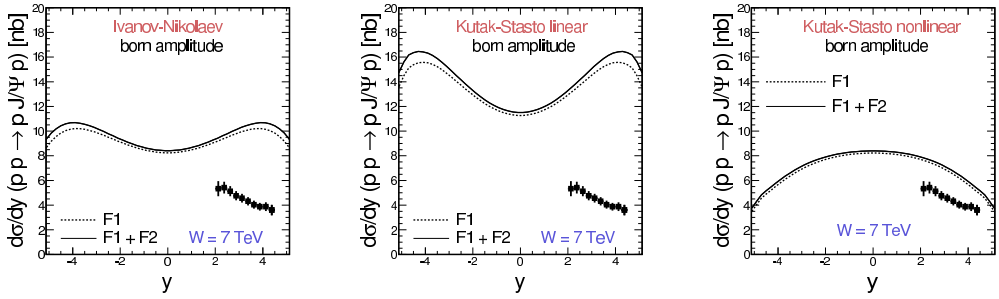

Figure 6. J/ψ rapidity distribution calculated with the Born amplitudes for three different UGDFs from the literature for $\sqrt{s} = 7\,\text{TeV}$. The dashed lines include contributions with Dirac F_1 electromagnetic form factor and the solid lines include in addition Pauli F_2 electromagnetic form factor. The new LHCb data points [3] are shown for comparison.

the Pauli electromagnetic form factor. In figure 9 we show both results with the standard absorption (elastic rescattering only) as well as with the absorption increased by a factor 1.4 to simulate inelastic (nucleon excitation) terms.

For completeness in figure 10 we present rapidity (left panel) and transverse momentum (right panel) distributions obtained using H1 parametrization [36] of the elementary $\gamma p \to J/\psi p$ cross section (see figure 5). A good agreement with the LHCb data precludes drawing definite conclusion about onset of saturation.

JHEP04(2015)159

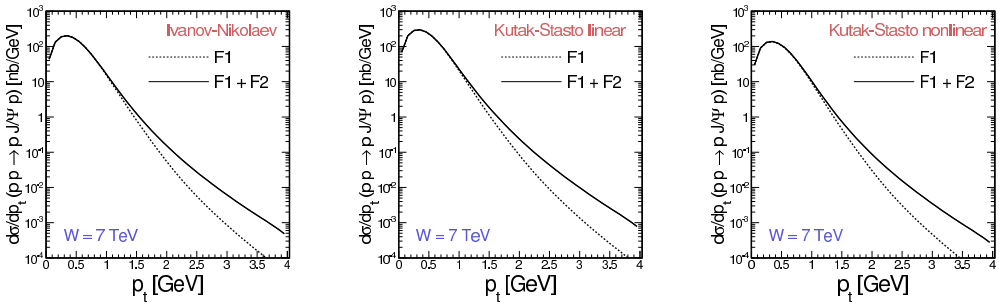

Figure 7. J/ψ transverse momentum distribution calculated with the Born amplitudes for three different UGDFs from the literature for $\sqrt{s} = 7\,\text{TeV}$. The dashed lines include contributions with Dirac F_1 electromagnetic form factor and the solid lines include in addition Pauli F_2 electromagnetic form factor.

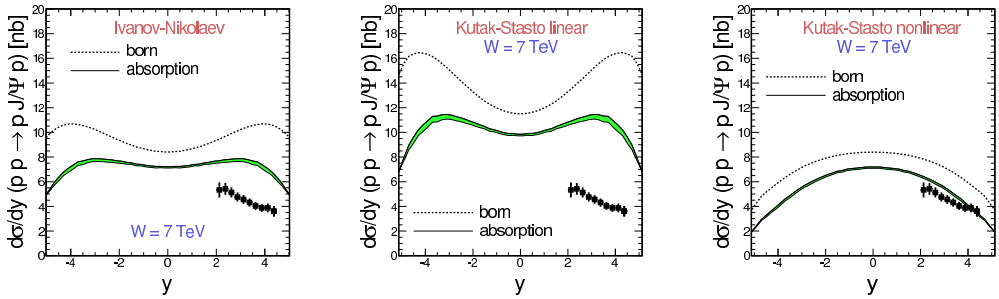

Figure 8. J/ψ rapidity distribution calculated with inclusion of absorption effects (solid line), compared with the Born result (dashed line) for $\sqrt{s} = 7\,\text{TeV}$. The new LHCb data points [3] are shown for comparison.

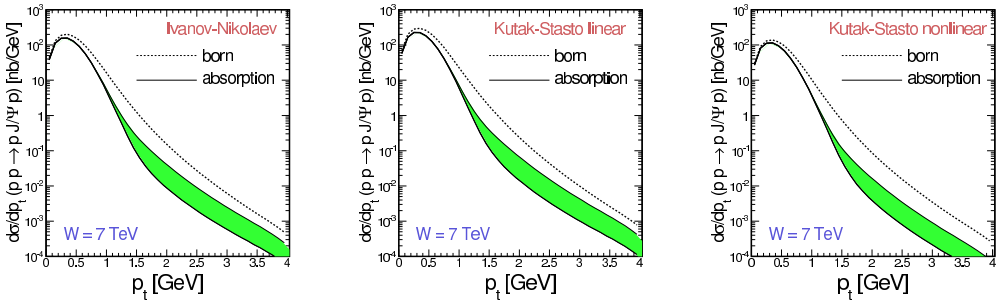

Figure 9. J/ψ transverse momentum distribution calculated with with absorption effects (solid line) and in the Born approximation for $\sqrt{s} = 7\,\text{TeV}$. The shaded (green online) band represents typical uncertainties in calculating absorption effects as described in the text.

JHEP04(2015)159

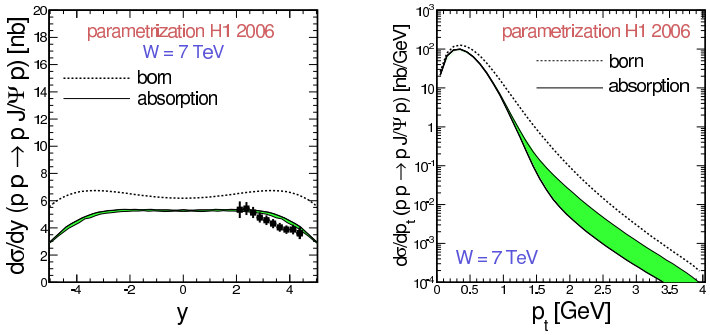

Figure 10. J/ψ rapidity and transverse momentum distributions calculated with the H1 parametrization [5, 36] of the elementary $\gamma p \to J/\psi p$ cross section for $\sqrt{s} = 7\,\text{TeV}$. The new LHCb data points [3] are shown for comparison.

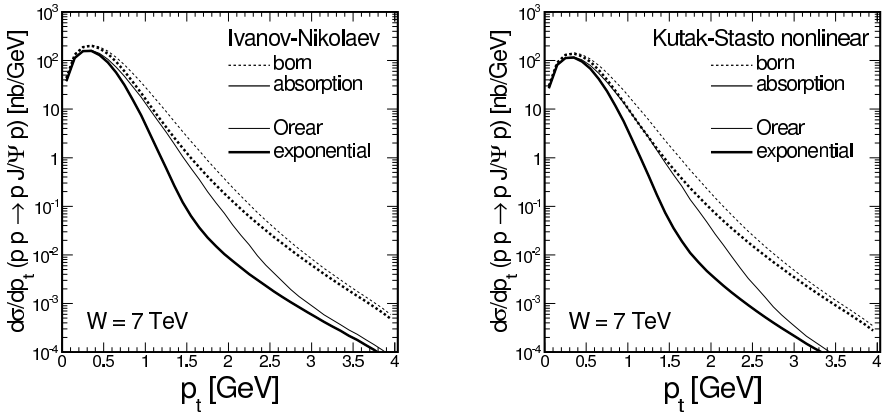

Figure 11. J/ψ transverse momentum distribution for exponential (thick lines) and Orear (thin lines) parametrizations for t-dependence of the elementary $\gamma p \to V p$ amplitude, without (dashed lines) and with (solid lines) absorption.

5.2 p_t-distributions for the Orear-parametrization

Now we wish to compare our J/ψ transverse momentum distributions for the $pp \to ppJ/\psi$ reaction at $\sqrt{s} = 7\text{TeV}$ for the exponential and the Orear distributions without and with absorption corrections (see figure 11). Somewhat harder distributions in transverse momentum are obtained with more realistic Orear distributions. The resulting distributions, being a convolution of the Orear and electromagnetic t distributions have rather complicated (nonexponential) shape. This shape may be important when extracting integrated cross sections form experimental data.

5.3 ψ' production

Now we shall proceed to the production of the excited charmonium state ψ'. In figure 12 we present total cross section for the $\gamma p \to \psi' p$ as a function of collision energy for the different UGDFs considered here. Almost all the UGDFs provide good description of new

JHEP04(2015)159

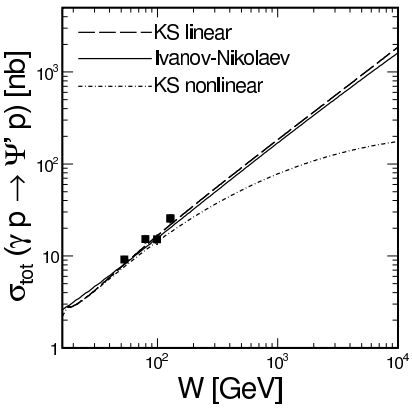

Figure 12. Total cross section for the $\gamma p \to \psi' p$ as a function of the subsystem energy together with the HERA data and pseudodata obtained by the LHCb collaboration. Three disfferent UGDFs have been used: Ivanov-Nikolaev (solid), Kutak-Stasto linear (dashed) and Kutak-Stasto nonlinear (dash-dotted). The experimental data are from ref. [11].

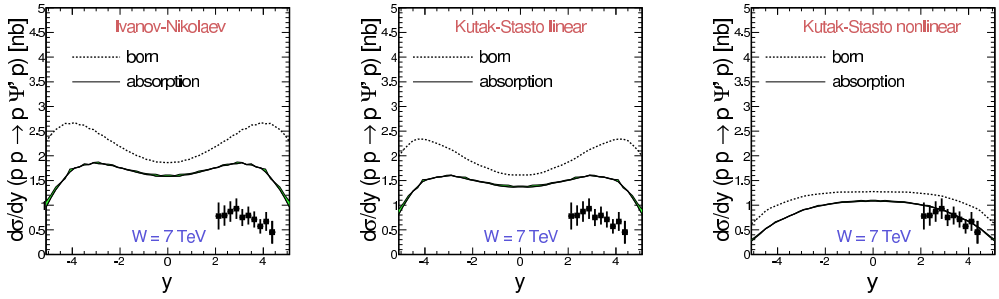

Figure 13. Rapidity distribution of ψ' calculated with inclusion of absorption effects (solid line), compared with the result when absorption effects are ignored (dotted line) for $\sqrt{s} = 7\,\text{TeV}$. The new LHCb data points [3] are shown for comparison.

HERA data [11]. The description seems better than in recent analysis in ref. [40] where the collinear gluon distribution fitted to the production of J/ψ [10] was used. Part of the success is due to explicit use of light cone wave functions which are not explicit in the collinear approximation as discussed above.

Now we turn to hadronic collisions. In figure 13 we present our predictions for rapidity distributions of ψ' again for different UGDFs. Results of our calculations are compared with recent LHCb data [3].

The role of Pauli electromagnetic form factor is quantified in figure 14. As for the ground state J/ψ the tensor coupling enhances the cross section at large meson transverse momenta.

The role of absorption effects is discussed in figure 15. The Born results are shown for comparison. The absorption effects lead to strong damping of of the cross section at large p_t's. This is a region where odderon exchange may show up.

JHEP04(2015)159

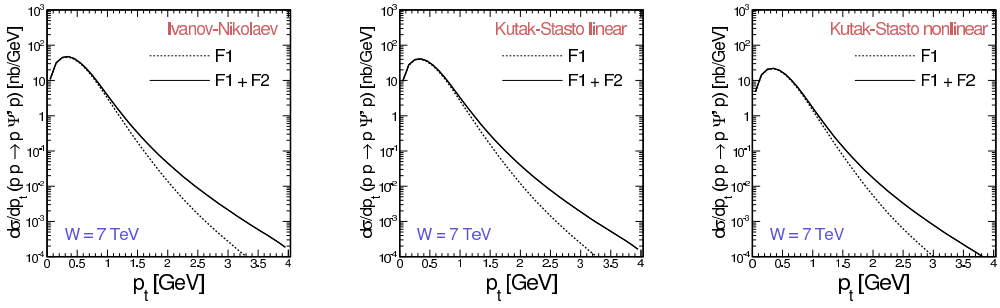

Figure 14. ψ' transverse momentum distribution calculated in the Born approximation with and without including Pauli electromagnetic form factor for $\sqrt{s} = 7\,\text{TeV}$.

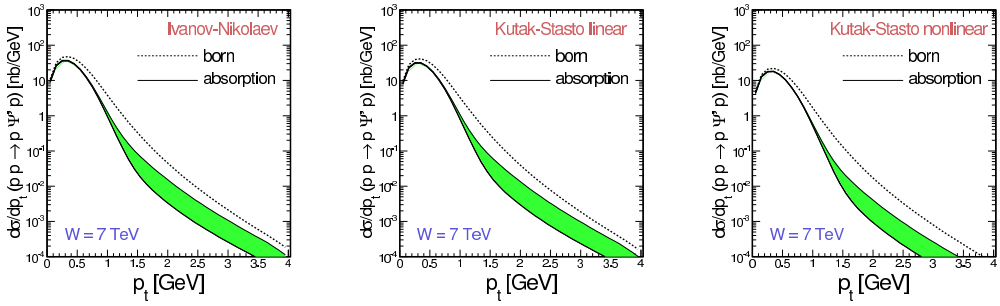

Figure 15. ψ' transverse momentum distribution calculated with absorption effects (solid line) and in the Born approximation (dashed line) for $\sqrt{s} = 7\,\text{TeV}$.

5.4 Dependence on the quarkonium wave functions

In figure 16 we wish to illustrate the charmonium wave function sensitivity. We show as an example rapidity distributions obtained with the Gaussian and Coulomb wave functions of quarkonia discussed in section 3. We remind that both sets of the wave functions by construction correctly describe branching fractions for the decay of the charmonia into dilepton pairs. Clearly the results depend not only on UGDF's but also on quarkonium wave functions. The combination of the Gaussian wave function and UGDF which includes nonlinear effects gives the best representation of the LHCb data [3]. So far the issue of the wave function influence for the $pp \to ppV$ reaction was, in our opinion, not sufficiently emphasized in the literature.

The ratio of the cross section for the production of the ψ' meson to that for the J/ψ meson is shown as a function of meson rapidity in figure 17. The data points for the ratio were obtained from the experimental data points for rapidity distributions from ref. [3]. The Gaussian wave functions well describe the so-obtained experimental data, while the Coulomb wave functions completely fail to describe the data. The example shows that the ratio is very sensitive to the choice of the wave function set.

We wish to point out here that in the approach with collinear gluons the effect of the quarkonium wave functions are reduced to a coupling constant which is a reasonable

JHEP04(2015)159

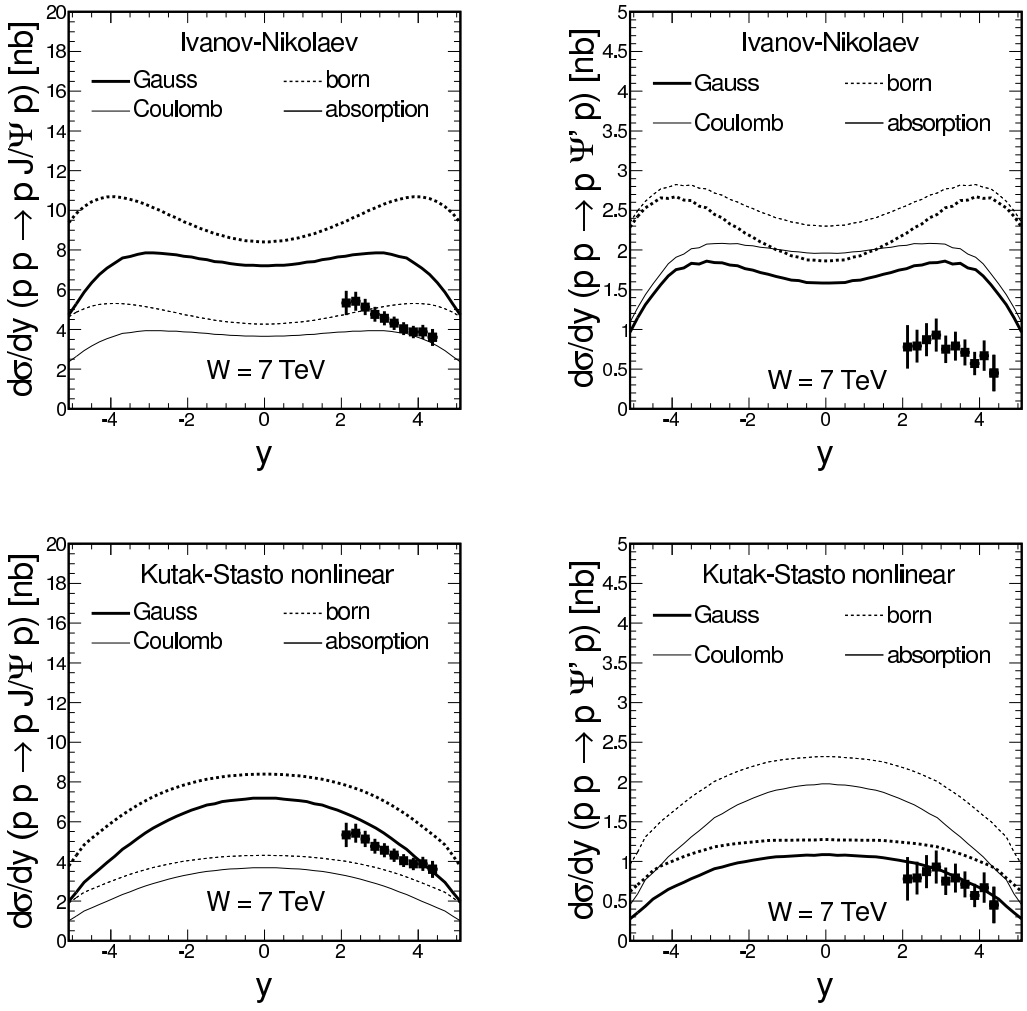

Figure 16. Rapidity distributions of J/ψ and ψ' mesons for Gaussian and Coulomb quarkonium wave functions.

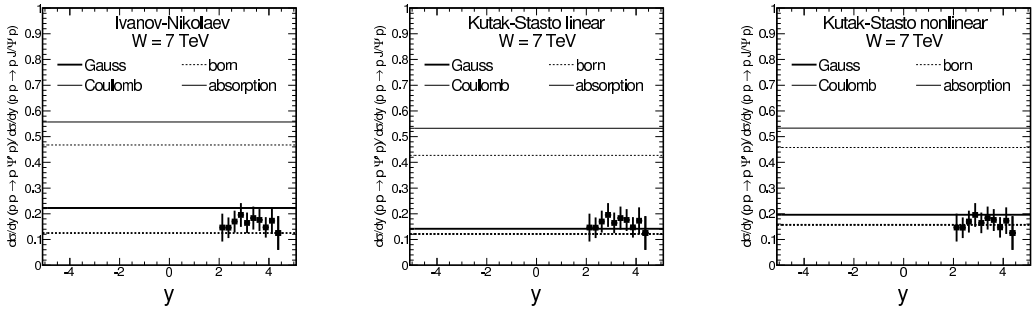

Figure 17. The ratio of the cross sections $\frac{d\sigma}{dy}(pp \to p\Psi' p)/\frac{d\sigma}{dy}(pp \to pJ/\Psi p)$ as a function of meson rapidity. The lines show results with Gaussian and Coulomb wave functions without and with absorption effects.

JHEP04(2015)159

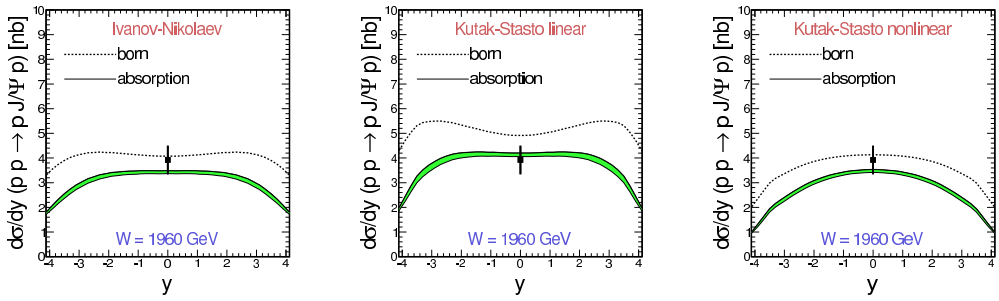

Figure 18. J/ψ rapidity distribution calculated with inclusion of absorption effects (solid line), compared with the Born result (dashed line) for $\sqrt{s} = 1.96\,\text{TeV}$. The CDF data point [1] is shown for comparison.

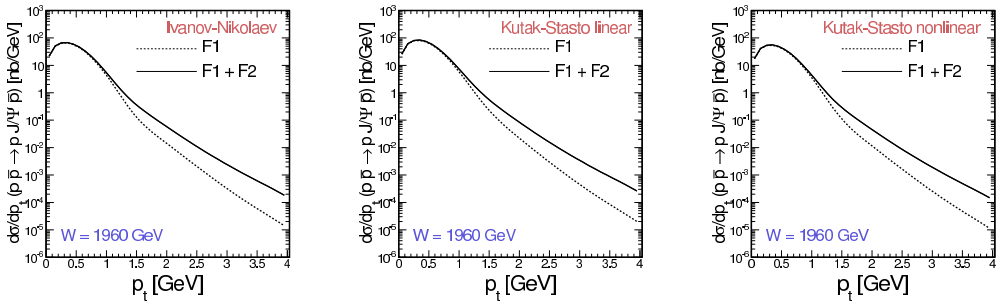

Figure 19. J/ψ transverse momentum distribution calculated with the Born amplitudes for three different UGDFs from the literature for $\sqrt{s} = 1.96\,\text{TeV}$. The dashed lines include contributions with Dirac F_1 electromagnetic form factor and the solid lines include in addition Pauli F_2 electromagnetic form factor.

approximation provided the relative velocity of quark and antiquark in the quarkonium wave function is small $v \ll 1$. This approximation should be better for heavier quarkonia such as Υ and its excited states and perhaps too crude for charmonia. One may expect that in a near future one could check this approach for the production of the members of the Υ family when the corresponding data of LHCb will be available. In the case of bottomonium production one is sensitive to the region of gluon x (longitudinal momentum fractions) which was already tested in other high-energy processes.

5.5 J/ψ and ψ' production at the Tevatron

In this section for completeness we present also results for the Tevatron. We repeat the same presentation as for the LHC. In figure 18 we show distribution in rapidity of J/ψ. All UGDFs considered here describe the CDF data point if the absorption effects are included.

In the next figure (figure 19) we demonstrate the role of the Pauli form factor on the J/ψ transverse momentum distribution. The distributions for the Tevatron (larger x values of the gluon distribution) drop much quicker than those for the LHC (lower x values of the gluon distribution). The role of absorption is presented in figure 20.

JHEP04(2015)159

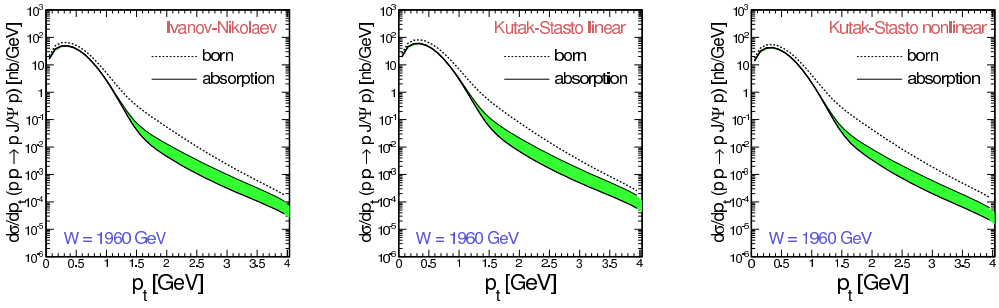

Figure 20. J/ψ transverse momentum distribution calculated with absorption effects (solid line) and in the Born approximation (dashed line).

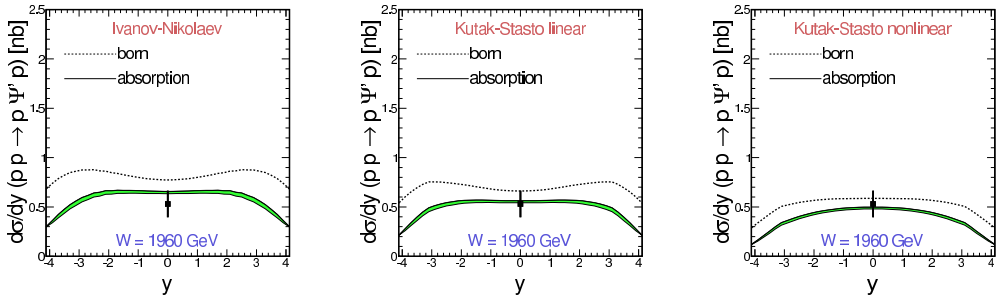

Figure 21. Rapidity distribution of ψ' calculated with inclusion of absorption effects (solid line), compared with the result when absorption effects are ignored (dotted line) for $\sqrt{s} = 1.96\,\text{TeV}$. The CDF data point [1] is shown for comparison.

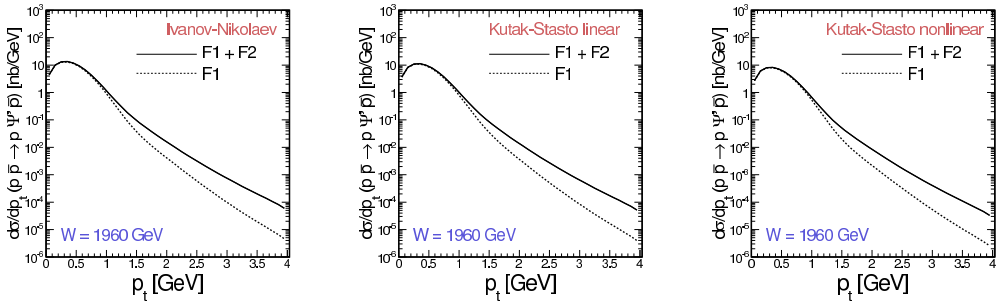

Figure 22. ψ' transverse momentum distribution calculated in the Born approximation with and without including Pauli electromagnetic form factor for $\sqrt{s} = 1.96\,\text{TeV}$.

The same distributions but for exclusive ψ' production are shown in figures 21, 22, 23. The shape of the distributions is very similar as for the J/ψ meson. The corresponding cross section is, however, much smaller. Again we nicely describe the Tevatron experimental point at midrapidity.

Summarizing the situation at the Tevatron, we nicely describe experimental data points at midrapidity both for exclusive J/ψ and ψ' production which gives further credibility to our approach.

JHEP04(2015)159

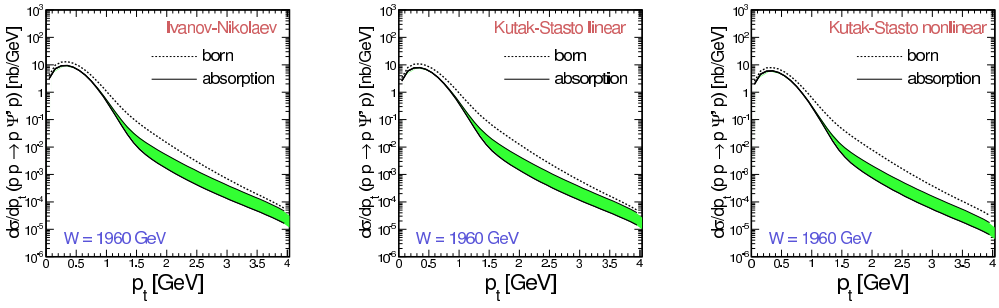

Figure 23. ψ' transverse momentum distribution calculated with absorption effects (solid line) and in the Born approximation (dashed line) for $\sqrt{s} = 1.96\,\text{TeV}$.

6 Conclusions

In the present paper we have reconsidered exclusive production of J/ψ meson in the $\gamma p \to J/\psi p$ and $pp \to ppJ/\psi$ reactions within the k_t-factorization formalism. First the total cross section for the $\gamma p \to J/\psi p$ reaction was calculated as a function of the subsystem energy and confronted with the HERA data for three different unintegrated distributions from the literature. We have focussed on the dependence of the cross section for the $\gamma p \to J/\psi p$ at intermediate-t ($\sim 1\,\text{GeV}^2$). The HERA data indicate that the always used exponential parametrization may be not sufficient. We have proposed to use a 'streched exponential' parametrization which better describes the large-t region and coincides with the exponential parametrization in small-t region. Such a parametrization is more adequate when focussing on larger transverse momenta of charmonia produced in proton-proton collisions.

In comparison to our earlier calculations in the past [5] in the present paper we have taken into account both the coupling of photons via spin-conserving vector coupling with F_1 Dirac electromagnetic form factor as well as spin-flipping tensor coupling with F_2 Pauli electromagnetic form factor for the $pp \to pJ/\psi p$ and $pp \to p\psi' p$ reactions. The theoretical approach used here allows to calculate many differential distributions for the three-body reaction $pp \to ppJ/\psi$. We have calculated not only J/ψ rapidity distribution but also distributions in J/ψ transverse momentum and distributions in four-momenta squared t_1 or t_2. The strength of the tensor coupling is quantified by Pauli electromagnetic form factor F_2. The tensor coupling is important for large $|t_1|$ or $|t_2|$ and as a consequence also for large transverse momenta of J/ψ. We have also carefully discussed the role of soft rescatterings which leads to a shape deformation of all distributions in contrast to commonly used uniform factor known as gap survival factor. The uncertainties related to the absorption effects have been discussed. We have shown that inclusions of inelastic rescatterings leads to further significant damping of the cross section at the large transverse momenta of J/ψ and ψ'.

Our calculations have been performed for different unintegrated gluon distributions used previously in the literature. The best agreement with the recent LHCb collaboration data has been achieved with UGDF which incorporates nonlinear effects in its evolution. This suggests an onset of saturation effects, especially for large J/ψ rapidities. Since a simple parametrization of the experimental cross section for $\gamma p \to J/\psi$ reaction also leads

JHEP04(2015)159

to a relatively good description of the LHCb data no definite conclusion on the onset of saturation can be drawn.

We have shown that Gaussian wave functions of vector charmonia much better describe the LHCb collaboration data than the Coulomb wave functions. This was demonstrated by presenting the ratios of cross sections for ψ' and J/ψ.

We have presented our results also for the Tevatron. A good agreement with the CDF experimental data point at the midrapidity for both J/ψ and ψ' has been achieved.

In the future we plan to find a phenomenological UGDF which simultaneusly describes the F_2 deep-inelastic structure function data and the LHCb collaboration data for semi-exclusive production of J/ψ. Then the photonic-inelastic contributions (the exchanged photon leaves the remaining system in an excited state) must be taken into account in the analysis in a similar fashion as recently done for $\mu^+\mu^-$ semi-exclusive production [41]. This clearly goes beyond the scope of the present paper.

Acknowledgments

We would like to thank to Ronan McNulty for a discussion of the LHCb data. This work was partially supported by the Polish MNiSW grant DEC-2011/01/B/ST2/04535 as well as by the Centre for Innovation and Transfer of Natural Sciences and Engineering Knowledge in Rzeszów.

Open Access. This article is distributed under the terms of the Creative Commons Attribution License (CC-BY 4.0), which permits any use, distribution and reproduction in any medium, provided the original author(s) and source are credited.

References

[1] CDF collaboration, T. Aaltonen et al., *Observation of exclusive charmonium production and $\gamma + \gamma$ to $\mu^+\mu^-$ in $p\bar{p}$ collisions at $\sqrt{s} = 1.96$ TeV*, *Phys. Rev. Lett.* **102** (2009) 242001 [arXiv:0902.1271] [INSPIRE].

[2] LHCb collaboration, *Exclusive J/ψ and $\psi(2S)$ production in pp collisions at $\sqrt{s} = 7$ TeV*, *J. Phys.* **G 40** (2013) 045001 [arXiv:1301.7084] [INSPIRE].

[3] LHCb collaboration, *Updated measurements of exclusive J/ψ and $\psi(2S)$ production cross-sections in pp collisions at $\sqrt{s} = 7$ TeV*, *J. Phys.* **G 41** (2014) 055002 [arXiv:1401.3288] [INSPIRE].

[4] S.R. Klein and J. Nystrand, *Photoproduction of quarkonium in proton proton and nucleus nucleus collisions*, *Phys. Rev. Lett.* **92** (2004) 142003 [hep-ph/0311164] [INSPIRE].

[5] W. Schäfer and A. Szczurek, *Exclusive photoproduction of J/psi in proton-proton and proton-antiproton scattering*, *Phys. Rev.* **D 76** (2007) 094014 [arXiv:0705.2887] [INSPIRE].

[6] L. Motyka and G. Watt, *Exclusive photoproduction at the Tevatron and CERN LHC within the dipole picture*, *Phys. Rev.* **D 78** (2008) 014023 [arXiv:0805.2113] [INSPIRE].

[7] A. Bzdak, L. Motyka, L. Szymanowski and J.-R. Cudell, *Exclusive J/ψ and Υ hadroproduction and the QCD odderon*, *Phys. Rev.* **D 75** (2007) 094023 [hep-ph/0702134] [INSPIRE].

JHEP04(2015)159

[8] V.P. Goncalves and M.V.T. Machado, *Vector meson production in coherent hadronic interactions: an update on predictions for RHIC and LHC*, *Phys. Rev.* **C 84** (2011) 011902 [arXiv:1106.3036] [INSPIRE].

[9] M.B. Gay Ducati, M.T. Griep and M.V.T. Machado, *Exclusive photoproduction of J/ψ and $\psi(2S)$ states in proton-proton collisions at the CERN LHC*, *Phys. Rev.* **D 88** (2013) 017504 [arXiv:1305.4611] [INSPIRE].

[10] S.P. Jones, A.D. Martin, M.G. Ryskin and T. Teubner, *Probes of the small x gluon via exclusive J/ψ and Υ production at HERA and the LHC*, *JHEP* **11** (2013) 085 [arXiv:1307.7099] [INSPIRE].

[11] H1 collaboration, C. Alexa et al., *Elastic and proton-dissociative photoproduction of J/ψ mesons at HERA*, *Eur. Phys. J.* **C 73** (2013) 2466 [arXiv:1304.5162] [INSPIRE].

[12] A. Cisek, *Exclusive processes with large rapidity gaps in the formalism of unintegrated gluon distributions*, Ph.D. thesis, Henryk Niewodniczański Institute of Nuclear Physics Polish Academy of Sciences, Kraków Poland (2012).

[13] I.P. Ivanov, N.N. Nikolaev and A.A. Savin, *Diffractive vector meson production at HERA: from soft to hard QCD*, *Phys. Part. Nucl.* **37** (2006) 1 [hep-ph/0501034] [INSPIRE].

[14] I.P. Ivanov, *Diffractive production of vector mesons in deep inelastic scattering within k_t factorization approach*, Ph.D. thesis, Bonn University, Bonn Germany (2003) [hep-ph/0303053] [INSPIRE].

[15] A. Rybarska, W. Schäfer and A. Szczurek, *Exclusive photoproduction of Υ: from HERA to Tevatron*, *Phys. Lett.* **B 668** (2008) 126 [arXiv:0805.0717] [INSPIRE].

[16] A. Cisek, W. Schäfer and A. Szczurek, *Exclusive photoproduction of ϕ meson in $\gamma p \to \phi p$ and $pp \to p\phi p$ reactions*, *Phys. Lett.* **B 690** (2010) 168 [arXiv:1004.0070] [INSPIRE].

[17] M.G. Ryskin, *Diffractive J/ψ electroproduction in LLA QCD*, *Z. Phys.* **C 57** (1993) 89 [INSPIRE].

[18] W. Jaus, *Semileptonic decays of B and D mesons in the light front formalism*, *Phys. Rev.* **D 41** (1990) 3394 [INSPIRE].

[19] W. Jaus, *Relativistic constituent quark model of electroweak properties of light mesons*, *Phys. Rev.* **D 44** (1991) 2851 [INSPIRE].

[20] I.P. Ivanov and N.N. Nikolaev, *Diffractive S and D wave vector mesons in deep inelastic scattering*, *JETP Lett.* **69** (1999) 294 [hep-ph/9901267] [INSPIRE].

[21] J. Orear, *Transverse momentum distribution of protons in p-p elastic scattering*, *Phys. Rev. Lett.* **12** (1964) 112 [INSPIRE].

[22] L.A. Harland-Lang, V.A. Khoze and M.G. Ryskin, *Modelling exclusive meson pair production at hadron colliders*, *Eur. Phys. J.* **C 74** (2014) 2848 [arXiv:1312.4553] [INSPIRE].

[23] ZEUS collaboration, S. Chekanov et al., *Exclusive photoproduction of J/ψ mesons at HERA*, *Eur. Phys. J.* **C 24** (2002) 345 [hep-ex/0201043] [INSPIRE].

[24] A.P. Trawiński, S.D. Głazek, S.J. Brodsky, G.F. de Téramond and H.G. Dosch, *Effective confining potentials for QCD*, *Phys. Rev.* **D 90** (2014) 074017 [arXiv:1403.5651] [INSPIRE].

[25] T. Gutsche, V.E. Lyubovitskij, I. Schmidt and A. Vega, *Light-front potential for heavy quarkonia constrained by the holographic soft-wall model*, *Phys. Rev.* **D 90** (2014) 096007 [arXiv:1410.3738] [INSPIRE].

JHEP04(2015)159

[26] T. Peng and B.-Q. Ma, *Heavy quarkonium $2S$ states in light-front quark model*, *Eur. Phys. J.* **A 48** (2012) 66 [arXiv:1204.0863] [INSPIRE].

[27] S.D. Glazek and J. Mlynik, *Boost-invariant Hamiltonian approach to heavy quarkonia*, *Phys. Rev.* **D 74** (2006) 105015 [hep-th/0606235] [INSPIRE].

[28] N.N. Nikolaev, *Quantum mechanics of color transparency*, *Comments Nucl. Part. Phys.* **21** (1992) 41 [INSPIRE].

[29] B.Z. Kopeliovich, J. Nemchick, N.N. Nikolaev and B.G. Zakharov, *Novel color transparency effect: scanning the wave function of vector mesons*, *Phys. Lett.* **B 309** (1993) 179 [hep-ph/9305225] [INSPIRE].

[30] J. Nemchik, N.N. Nikolaev, E. Predazzi and B.G. Zakharov, *Color dipole phenomenology of diffractive electroproduction of light vector mesons at HERA*, *Z. Phys.* **C 75** (1997) 71 [hep-ph/9605231] [INSPIRE].

[31] J. Hüfner, Y. Ivanov, B.Z. Kopeliovich and A.V. Tarasov, *Photoproduction of charmonia and total charmonium proton cross-sections*, *Phys. Rev.* **D 62** (2000) 094022 [hep-ph/0007111] [INSPIRE].

[32] L. Frankfurt, W. Koepf and M. Strikman, *Diffractive heavy quarkonium photoproduction and electroproduction in QCD*, *Phys. Rev.* **D 57** (1998) 512 [hep-ph/9702216] [INSPIRE].

[33] CDF collaboration, F. Abe et al., *Measurement of small angle $\bar{p}p$ elastic scattering at $\sqrt{s} = 546$ GeV and 1800 GeV*, *Phys. Rev.* **D 50** (1994) 5518 [INSPIRE].

[34] TOTEM collaboration, G. Antchev et al., *Measurement of proton-proton elastic scattering and total cross-section at $\sqrt{s} = 7$ TeV*, *Europhys. Lett.* **101** (2013) 21002 [INSPIRE].

[35] H1 collaboration, C. Adloff et al., *Diffractive photoproduction of $\psi(2S)$ mesons at HERA*, *Phys. Lett.* **B 541** (2002) 251 [hep-ex/0205107] [INSPIRE].

[36] H1 collaboration, A. Aktas et al., *Elastic J/ψ production at HERA*, *Eur. Phys. J.* **C 46** (2006) 585 [hep-ex/0510016] [INSPIRE].

[37] I.P. Ivanov and N.N. Nikolaev, *Anatomy of the differential gluon structure function of the proton from the experimental data on $F_{2p}(x, Q^2)$*, *Phys. Rev.* **D 65** (2002) 054004 [hep-ph/0004206] [INSPIRE].

[38] K. Kutak and A.M. Staśto, *Unintegrated gluon distribution from modified BK equation*, *Eur. Phys. J.* **C 41** (2005) 343 [hep-ph/0408117] [INSPIRE].

[39] A. Cisek, P. Lebiedowicz, W. Schafer and A. Szczurek, *Exclusive production of ω meson in proton-proton collisions at high energies*, *Phys. Rev.* **D 83** (2011) 114004 [arXiv:1101.4874] [INSPIRE].

[40] S.P. Jones, A.D. Martin, M.G. Ryskin and T. Teubner, *Predictions of exclusive $\psi(2S)$ production at the LHC*, *J. Phys.* **G 41** (2014) 055009 [arXiv:1312.6795] [INSPIRE].

[41] G.G. da Silveira, L. Forthomme, K. Piotrzkowski, W. Schäfer and A. Szczurek, *Central $\mu^+\mu^-$ production via photon-photon fusion in proton-proton collisions with proton dissociation*, *JHEP* **02** (2015) 159 [arXiv:1409.1541] [INSPIRE].

JHEP04(2015)159